Chronic refined low-fat diet consumption reduces cholecystokinin satiation in rats

Mathilde Guerville, M Kristina Hamilton, Charlotte C Ronveaux, Sandrine Ellero-Simatos, Helen E Raybould, Gaëlle Boudry

Chronic refined low fat diet consumption reduces cholecystokinin satiation in rats.

Mathilde Guerville[1], M. Kristina Hamilton[2], Charlotte C Ronveaux[2], Sandrine Ellero-Simatos[3], Helen E Raybould[2] and Gaëlle Boudry[1]

[1] Institut Numecan INRA INSERM Univ Rennes 1, Domaine de la Prise, Saint-Gilles, France

[2] Dept of Anatomy, Physiology and Cell Biology, UC Davis School of Veterinary Medicine, Davis, CA

[3] Toxalim (Research Centre in Food Toxicology), Université de Toulouse, INRA, ENVT, INP-Purpan, UPS, Toulouse, France.

SHORT TITLE: Refined diet reduces CCK satiation in rats

Corresponding author:

Dr Gaëlle Boudry

Institut NuMeCan, INRA INSERM Univ Rennes 1

Domaine de la Prise

35590 Saint-Gilles

France

Gaelle.Boudry@inra.fr

Abstract

Purpose: Reduced ability of cholecystokinin (CCK) to induce satiation contributes to hyperphagia and weight gain in high fat / high sucrose (HF/HS) diet-induced obesity, and has been linked to altered gut microbiota. Rodent models of obesity use chow or low fat (LF) diets as control diets; the latter has been shown to alter gut microbiota and metabolome. We aimed to determine whether LF diet consumption impacts CCK satiation in rats and if so, whether this is prevented by addition of inulin to LF diet.

Methods: Rats (n=40) were fed for 8 weeks a chow diet (chow) or low fat (10%) or high fat / high sucrose (45 and 17%, respectively) refined diets with either 10% cellulose (LF and HF/HS) or 10% inulin (LF-I and HF/HS-I). Caecal metabolome was assessed by ^{1}H-NMR-based metabolomics. CCK satiation was evaluated by measuring the suppression of food intake after intraperitoneal CCK injection (1 or 3 µg/kg).

Results: LF diet consumption altered the caecal metabolome, reduced caecal weight and increased IAP activity, compared to chow. CCK-induced inhibition of food intake was abolished in LF diet fed rats compared to chow-fed rats, while HF/HS diet-fed rats responded only to the highest CCK dose. Inulin substitution ameliorated caecal atrophy, reduced IAP activity and modulated caecal metabolome, but did not improve CCK-induced satiety in either LF or HF/HS fed rats.

Conclusions: CCK signaling is impaired by LF diet consumption, highlighting that caution must be taken when using LF diet until a more suitable refined control diet is identified.

Keywords: obesity, gut-brain axis, metabolomics, vagal afferents, food intake

INTRODUCTION

The gastrointestinal tract releases more than 20 different hormones that contribute to the regulation of satiety and hunger. The most extensively studied satiating hormone is cholecystokinin (CCK), which is synthesized and secreted in the duodenum in response to the presence of fat and protein in the lumen [1, 2]. In rodents, CCK acts synergistically with leptin to enhance the activity of vagal afferent neurons (VAN), relaying information to the nucleus of the solitary tract (NTS) and then to the hypothalamus [3]. Integration of this signal leads to reduction of food intake and meal termination [2, 4]. Regulation of food intake by the CCK-leptin system is impaired in certain conditions such as diet-induced obesity (DIO) [5, 6]. Indeed DIO-rodents are insensitive to low doses of CCK [5]. Decreased sensitivity to satiating signals may ultimately lead to hyperphagia and weight gain enhancement. Thus, understanding the mechanisms leading to altered CCK sensitivity is of upmost importance in the context of obesity and overweight pandemic. Leptin-resistance of VAN has been described as the causal mechanism of this loss of sensitivity to CCK [5]. Yet the full mechanisms leading to VAN leptin-resistance and ultimately decreased satiation signals are still not fully described.

Most obesity studies using DIO rodent models examined differences between a control group fed a chow diet and animals fed a refined high fat/high sucrose (HF/HS) diet that provides 4 to 6 times more fat than the chow diet [7]. Chow diet is composed of a large array of unrefined plant and animal products. Conversely, HF/HS diet is processed with purified ingredients, each of them providing one main macronutrient or micronutrient. Many differences can be found between these diets: the nature and quantity of protein, fat, sugars and dietary fibers as well as the level of micronutrients [7, 8]. Hence, when comparing the effects of HF/HS diet to that of chow, the impact of increased dietary fat is confounded with the effects of other components that differ between the diets [7, 8]. Refined low fat (LF) diet has also been widely used in DIO studies as control diet. However, using various diets and animal models, Chassaing et al observed that switching from chow to refined diets, irrespective of dietary fat content or protein nature, leads to altered gut homeostasis with major atrophy of the large intestine [9]. Among

the most striking effects was the dramatic change in caecal metabolome in rats fed a refined LF diet compared to chow-fed ones as demonstrated by the use of ^{1}H-RMN [9]. This suggests that refined LF diet consumption by itself induces gut microbiota dysbiosis. This effect of refined LF diet upon gut microbiota and gut morphology was recently confirmed by Dalby et al. [10]. Interestingly, substituting inulin, a soluble fiber, for cellulose in refined LF diet improved caecal metabolomic profile and prevented intestinal atrophy [9].

One consistent observation in the literature is that altered VAN-mediated gut-brain communication is associated with dysbiosis and altered gut homeostasis. Indeed, using antibiotics to manipulate HF/HS diet-induced change in gut microbiota composition in rats, a recent study demonstrated that gut microbiota dysbiosis induces withdrawal of VAN from the gut and the NTS and increases expression of inflammatory markers in VAN [11]. Microglia activation in the nodose ganglia is also associated with altered gut barrier function and intestinal inflammation in rats fed high sucrose diets [12]. Moreover, lipopolysaccharides (LPS), gut bacterial components that translocate to the blood in DIO [13], have been identified as potential triggers of VAN dysfunction *in vitro* [14] and *in vivo* [15]. Taken together these data suggest that altered host-microbiota interactions in obesity participates in the disturbances of VAN-mediated CCK signaling to the brain[16]. We therefore hypothesized that because of the major effects of refined LF diet upon gut microbiota and gut morphology recently described, LF diet consumption itself would alter CCK signaling compared to a chow diet, independently of dietary fat content. We also hypothesized that by preventing LF diet-induced dysbiosis and gut atrophy, addition of inulin to a LF diet would improve vagal signaling to the brain and constitute a proper control diet that could be used for further study. We therefore formulated 4 refined diets differing in fat and sucrose content and nature of fiber: low-fat cellulose (LF), low-fat inulin (LF-I), high-fat/high sucrose cellulose (HF/HS) and high-fat/high sucrose inulin (HF/HS-I) and fed these diets to rats for 8 weeks. We evaluated gut microbiota metabolome and gut morphology as well as the ability of CCK to induce meal termination in rats fed these refined diets compared to that of a group of rats fed chow.

MATERIAL AND METHODS

Animals

Male Wistar rats (9-week old, 280-370g Harlan San Diego, n=40) were maintained and handled in accordance with protocols approved by the Institutional Animal Care and Use Committee (University of California, Davis, USA). All animals were housed individually at 22°C with a 12:12 hour light-dark in 435 x 290 x 150 mm polycarbonate rat cage. Body weight and food intake were measured three times a week. Food intake was measured by weighing the remaining food in the cage lid top after careful examination of the cage to collect crumbles. Rats were fed a chow diet (Chow; Purina Lab Diet 5001 rodent diet, 3.4 kcal/g, Table 1) for two weeks during acclimation to the animal facility. Rats were then split into 5 weight-matched groups and fed either chow, low fat (LF; Research diets D12450H, 3.7 kcal/g, 10% Cellulose, Table 2), LF-inulin (LF-I; Research diets, 10% Inulin, 3.8 kcal/g, Table 2), high fat (HF/HS; Research diets D12451, 4.5 kcal/g, 10% Cellulose, Table 2) or HF/HS-inulin (HF/HS-I; Research diets, 4.7 kcal/g, 10% Inulin, Table 2) diets for 8 weeks (n=8 per group). Energy intake and feed conversion ratio (kcal ingested / weight gain) were calculated according to the nutritional information given by the supplier. Inulin was purchased from Beneo (Orafti® GR; Belgium) and supplemented into the LF and HF/HS diets by Research Diets. Inulin was extracted from chicory root and had an average chain length >10.

CCK sensitivity assessment

After 6 weeks on respective diets, rat sensitivity to the satiating effect of CCK was tested. Experiments were performed at the onset of the dark phase. Rats were fasted on wire-bottom cages for 12h during the light phase. At the onset of the dark phase, CCK (octapeptide, sulfated, Bachem, Torrance, CA, 1µg or 3 µg/kg; i.p.) or saline (400 µL; i.p.) were administered. Food was placed in the cage and food intake recorded after 20 and 60 minutes. The dose of CCK was chosen based on previous work showing decreased sensitivity to CCK i.e. no satiating effect of the lowest CCK dose but intact effect of the highest dose in DIO (defined as

rats with significantly greater adiposity index than chow-fed rats) rats compared to chow-fed rats [14]. All rats received vehicle and CCK doses randomly, with a minimum of 48 hours between each fast.

Tissue collection

After 8 weeks on respective diets, rats were fasted overnight then injected leptin (80 µg/kg i.p., n=4 per group) or saline (400µL, n=4 per group). They were euthanized 2 hrs later by cardiac puncture under deep anesthesia induced by isoflurane. Plasma was obtained by centrifugation (4000rpm, 10 min, 4°C) and stored at -80°C. Fat pads were dissected (mesenteric fat corresponding to the whole mesentery, epididymal fat located around the epididymes and retroperitoneal fat around the kidneys) and weighed. Adiposity was calculated as the sum of fat pad weights / body weight * 100. Retroperitoneal fat sample (1 cm^3) was fixed in 4% buffered paraformaldehyde for 24hrs then processed for paraffin embedding. Caecum and luminal contents were snap frozen in liquid nitrogen and stored at -80°C. Nodose ganglia were dissected and immediately snap frozen in liquid nitrogen and stored at -80°C.

Intestinal alkaline phosphatase activity

After homogenization of caecal samples, the activity of alkaline phosphatase was assayed in caecal homogenates with commercial kits according the manufacturer's instructions (Sensolyte, Anaspec, San Jose, CA, USA).

Plasma LPS-binding protein

Lipopolysaccharide-binding protein (LBP) levels were measured in serum samples via ELISA kit according to manufacturer's recommendations (Biometec, Greifswald, Germany).

Histology of adipose tissue

Retroperitoneal fat samples of 4 rats per dietary group were cut (10µm). Sections were stained with hematoxylin and eosin and images were taken at 100x magnification using the MetaMorph

Basic v. 7.7.0. image-analyzer software on an Olympus BX61 microscope. The area of adipocytes was measured with Image J 1.42p digital imaging processing software. Each image was converted into a binary format, and the area of adipocytes for each sample was analyzed in six random microscopic fields. All measurements were done blinded for diet group.

Western blot PTP1b

Proteins from nodose ganglia were extracted with Tris-base EDTA buffer (1%Triton, 1% protease inhibitor, 1% Phosphatase inhibitor and 3%PMSF). Samples (5µg of protein) were loaded into precast 10% BisTris gels (Invitrogen NuPage) and migrated for 50 minutes at 200V. The proteins were transferred on a PDVF membrane (Biorad #162-0174 7.0cm x 8.5cm) for 1 h at 30V. Membrane was blocked using 10% BSA in PBS for 1 h at room temperature. Anti-protein tyrosine phosphatse 1b (PTP1b) (Rabbit, Abcam, ab189179) was diluted at 1:500 and anti-GADPH (Rabbit, Cell Signalling, 14C10) was used as a loading control. Primary antibodies were applied on the membrane and developed on separate but consecutive days. Antibodies were incubated for 1 h at room temperature and then overnight at 4°C. The membrane was imaged using ECL substrate (Thermo Scientific) and with ChemiDoc XRS Imager (BioRad, Hercules, CA). The membrane was analyzed by Image Lab version 5.0 software (Hercules, CA)

^{1H} NMR metabolomics

Caecal extracts for NMR spectroscopy were prepared by mixing 50 mg of the caecal content with 500 µL of phosphate buffer (0.2 M, pH 7.4) containing 90% D_2O, 1% (w/v) of sodium 3-(trimethylsilyl) propionate (TSP), and 0.3 mM NaN_3. After vortexing, each sample was subjected to a freeze−thaw cycle in liquid nitrogen and subsequently homogenized with a tissue lyser (QIAGEN, Hilden, Germany) at 20 Hz for 40 s followed by centrifugation at 10000×g for 10 min at 4°C. The supernatants were collected, and the remaining pellet was extracted once more as described above. Supernatants obtained from the two extractions

were combined and centrifuged at 10000×g for 10 min at 4°C. A total of 600 µL of supernatant was transferred into an NMR tube (outer diameter, 5 mm) pending NMR analysis. All ^{1}H-NMR spectra were obtained on a Bruker DRX-600-Avance NMR spectrometer (Bruker, Wissembourg, France) on the AXIOM metabolomics platform (MetaToul, Toulouse, France) operating at 600.13 MHz for ^{1}H resonance frequency using an inverse detection 5-mm ^{1}H-^{13}C-^{15}N cryoprobe attached to a cryoplatform (the preamplifier cooling unit). The ^{1}H-NMR spectra were acquired at 300K using the Carr-Purcell-Meiboom-Gill spin-echo pulse sequence with pre-saturation and a total spin-echo delay (2nτ) of 100 ms. A total of 128 transients were collected into 64,000 data points using a spectral width of 12 ppm, a relaxation delay of 2.5 s, and an acquisition time of 2.28 s. Data were analyzed by applying an exponential window function with a 0.3-Hz line broadening prior to Fourier transformation. The resultant spectra were phased, baseline corrected, and calibrated to TSP (δ 0.00) manually using Mnova NMR (v9.0, Mestrelab Research). The spectra were subsequently imported into MatLab (R2014a, MathsWorks, Inc.) All data were analyzed using full-resolution spectra. The region containing the water resonance (δ 4.6–5.2ppm) was removed, and the spectra were normalized to the probabilistic quotient [17] and aligned using a previously published function [18].

Data were mean-centered prior to analysis using orthogonal projection on latent structure-discriminant analysis (O-PLS-DA). ^{1}H-NMR data were used as independent variables (X matrix) and regressed against a dummy matrix (Y matrix) indicating the class of samples. O-PLS-derived model was evaluated for goodness of prediction (Q^2Y value) using 8-fold cross-validation. The reliability of each model was established using a permutation test of the Y vector (1000 permutations) in order to determine a p-value for each Q^2Y. To identify metabolites responsible for discrimination between the dietary groups, the O-PLS-DA correlation coefficients (r^2) were calculated for each variable and back-scaled into a spectral domain, so that the shape of NMR spectra and the sign of the coefficients were preserved[19]. The weights of the variables were color-coded, according to the square of the O-PLS-DA correlation coefficients. Correlation coefficients extracted from significant models were filtered

so that only significant correlations above the threshold defined by Pearson's critical correlation coefficient ($P < 0.05$; $|r| > 0.71$) were considered significant. For illustration purposes, the area under the curve of several signals of interest was integrated and statistical significance was tested using univariate tests.

Statistical analysis

Statistical analysis was performed on GraphPad Prism software (v5, San Diego, CA USA) and data were expressed as means +/- SEM. Significance was determined by one-way ANOVA for cumulative energy intake, feed conversion ratio, liver weight, adiposity, caecal weight and IAP activity. For the CCK sensitivity assessment, the significance was determined by two-way ANOVA testing the effect of the CCK dose, diet and of the interaction between these two factors. For body weight, data were analyzed using two-way ANOVA testing the effect of time, diet and the interaction between those two factors. Finally, frequency of adipocyte size was analyzed using two-way ANOVA testing the diet, adipocyte size class and the interaction between factors.

RESULTS

LF and HF/HS diets had different effects on rat phenotype which were modulated by inulin

Rats fed HF/HS diet gained more weight compared to both chow and LF diet-fed rats during the 8-week feeding period (Fig. 1A), resulting in a greater body weight after 6, 7 and 8 weeks on the HF/HS diet (Fig. 1B). Substitution of inulin for cellulose in the HF/HS diet did not change rat weight gain after 8 weeks of diet consumption, with HF/HS-I diet-fed rats exhibiting body weight gain similar to that of HF/HS diet-fed rats and greater than that of chow, LF- and LF-I diet-fed rats (Fig. 1A and B).

Average daily energy intake of HF/HS diet-fed rats was greater at week 1 compared to that of the other dietary groups (Fig. 1C). Average daily energy intake was stable after 2 weeks and not different from that of the other groups. This resulted in a cumulative energy intake similar in HF/HS-diet and chow-fed rats (Fig. 1D). Feed conversion ratio (kcal/weight gain) was lower in HF/HS-diet fed rats compared to chow-fed rats (Fig. 1E). Average daily energy intake was not significantly different from that of chow-fed rats and stable after 2 weeks on refined diets (Fig. 1D). However, when expressed as cumulative energy intake, LF diet-fed rats exhibited a lower cumulative energy intake compared to chow and HF/HS diet-fed rats (Fig. 1D). They had a similar feed conversion ratio to that of HF/HS diet-fed rats (Fig. 1E). Inulin did not change caloric intake in LF-I diet-fed rats which exhibited lower cumulative food intake compared to chow-fed rats (Fig. 1C and D). A slight reduction in cumulative caloric intake was observed in HF/HS-I diet-fed rats compared to HF/HS-diet fed ones ($P=0.06$, Fig. 1D).

Plasma LBP was not different between chow- and refined diet-fed rats (Fig. 1F). However, LF-I diet-fed rats exhibited a significantly greater level of LBP compared to LF diet-fed ones (Fig. 1F).

Relative to chow-fed rats, HF/HS diet-fed rats exhibited marked adiposity with an increased adiposity index (Fig. 1G) characterized by elevated retroperitoneal, mesenteric and epididymal fat pad mass (data not shown). This increased adiposity was attributable at least in part to

adipocyte hypertrophy as demonstrated by the significant increase in the frequency of large adipocytes (size comprised between 8 and 10 000 µm²) and decrease in smaller ones (size comprised between 4 and 6 000 µm²) in HF diet-fed compared to chow-fed rats (Fig. 1H). Adiposity of LF diet-fed rats was not significantly different from that of chow or HF/HS diet-fed rats (Fig. 1G). However, adipocyte size distribution was slightly altered by LF diet consumption since the frequency of intermediate size adipocytes (size comprised between 6 and 8 000 µm²) was significantly increased and that of smaller adipocytes (size comprised between 4 and 6 000 µm²) decreased in LF diet- compared to chow-fed rats (Fig. 1H). Inulin did not change adiposity which was still greater in HF/HS-I-diet fed rats than chow-fed ones (Fig. 1G). Adipocyte size distribution in HF/HS-I diet-fed rats was not significantly different from that of HF/HS diet-fed ones but also not different from that of chow-fed ones, suggesting slight improvement of adipocyte hypertrophy. This improvement in adipocyte size distribution was visible in LF-I diet-fed rats which exhibited significant decrease in the frequency of adipocytes with a size between 6 and 8 000 µm² and significant increase in smaller adipocytes (4 - 6 000µm²) compared to LF-diet fed rats (Fig. 1H).

Liver weight was not impacted by any of the diets (data not shown).

LF and HF/HS diets had similar impacts on caecal metabolome, morphology and defense mechanisms, which were partially prevented by inulin

We investigated the diet-induced alterations in gut microbiota metabolome using ^{1}H-NMR based metabolomics in caecal extracts. Typical spectrum with identified metabolites is displayed in Suppl. Fig. 1.

The caecal metabolomic profile of chow-fed rats was significantly different from those of LF- or HF/HS diet-fed rats as demonstrated by the OPLS-DA scores showing clear clustering of chow-fed *vs* LF- or HF/HS diet-fed rats (Fig. 2A and Table 3). The caecal metabolomes of LF- and HF/HS diet-fed rats were not significantly different from each other, as reflected by the non-significant OPLS parameters (Table 3) and the non-separation of the 2 groups on the OPLS scores (Fig. 2B). OPLS models discriminating the caecal metabolic profiles from chow-

281 *vs*. LF diet-fed rats and chow- *vs*. HF/HS diet-fed rats were used to identify metabolites
282 responsible for the discrimination between metabolomes (Fig. 2C and D).
283 More specifically, we observed that consumption of LF or HF/HS diets had a minimal impact
284 on the caecal levels of bile acids and short chain fatty acids (Table 4). However, refined diets
285 consumption increased the caecal levels of many amino acids such as isoleucine, lysine, valine
286 in LF diet-fed rats and isoleucine in HF/HS-diet fed rats (Table 4). Similar trends for alanine,
287 aspartate and phenylalanine were also observed. Conversely, the levels of the valine
288 metabolite, α-keto-isovalerate, was decreased and that of 5-aminvalerate increased with LF
289 diet consumption (Table 4). A tendency for decreased levels of the aromatic amino acid
290 metabolite, 4-hydroxyphenylacetate (4-HPPA) in the caecum of LF diet-fed rats was observed.
291 Increased level of the ketone body β-hydroxybutyrate and a tendency for decreased level of
292 α-keto-glutarate were observed in the caecum of HF/HS diet-fed rats, with similar trends in LF
293 diet-fed rats (Table 4). The level of two unknown metabolites and of hypoxanthine was
294 decreased in rats fed the LF or HF/HS-diets (Table 4).
295 Addition of inulin to the refined diets impacted the caecal metabolome of LF diet-fed rats but
296 not of HF/HS-diet fed ones. The caecal metabolome of LF-I fed-rats was different from that of
297 both chow- and LF diet-fed rats as demonstrated by the clear separation of the 3 groups on
298 the O-PLSDA (Fig. 2E and Table 3) while that of HF/HS-I and HF/HS diet-fed rats were not
299 different (Fig. 2F and Table 3). Because of the strong difference between caecal metabolomic
300 profiles of chow- *vs.* refined diet-fed rats, we also analyzed metabolomic data after omitting
301 the chow-fed rat group. The OPLS model discriminating the 4 refined diets confirmed the
302 significant impact of inulin substitution on caecal metabolome, especially in the LF diet (Fig.
303 2G and Table 3). Metabolites responsible for the difference between LF- and LF-I diet-fed rat
304 caecal metabolomic profiles are displayed on Fig. 2F.
305 Specifically, inulin substitution increased the caecal content levels of butyrate (significant for
306 LF-I diet, Table 4). LF-I and HF/HS-I diet-fed rats had reduced caecal levels of isoleucine and
307 valine and increased levels of choline and hypoxanthine compared to LF and HF/HS diet-fed
308 rats, with the greatest effects seen in LF-I diet-fed rats. Inulin substitution tended to decrease

caecal levels of the ketone body β-hydroxybutyrate, to values closer to that of chow fed-rats (Table 4). Inulin had no effect on the variations in lysine, α-ketoisovalerate, trimethylamine and the two unknown compounds induced by LF- and HF/HS-diet consumption (Table 4). Surprisingly, inulin substitution enhanced the increase in aspartate and phenylalanine and the decrease in 4-HPPA caecal contents already observed with LF- and HF/HS-diet consumption. Moreover, it increased the level of alanine and tyrosine in the caecal content of LF-I and HF/HS-I diet-fed rats. Finally, glutamate level was increased and 5-aminovalerate level decreased in the caecal content of LF-I diet-fed rats (Table 4).

Consumption of LF and HF/HS diets induced gut atrophy with decreased caecal tissue weight in LF- and HF/HS diet-fed compared to chow-fed rats (Fig. 2I). Caecal atrophy was prevented by addition of inulin in the diets (Fig. 2I). We also evaluated the caecal activity of intestinal alkaline phosphatase (IAP) a key brush-border enzyme in the defense mechanisms of the mucosa which has been shown to be strongly induced in DIO and plays an essential role in intestinal homeostasis and health through interactions with the resident microbiota, diet and the gut[20]. Relative to chow-fed rats, LF diet-fed rats exhibited a 15-fold increase in caecal IAP activity (Fig. 2J). Caecal IAP activity was increased 7-fold in HF/HS diet-fed rats but this did not reach significance (Fig. 2J). The increase in IAP activity in the caecum induced by LF-diet consumption was prevented by addition of inulin (Fig. 2J)

LF and HF/HS diet-fed rats exhibited reduction in sensitivity to CCK and VAN leptin resistance, which were not improved by inulin

Chow-fed rats displayed decreased calorie intake during the first 20 min following administration of both doses of CCK (Fig. 3A and B), with no difference in calorie intake between the two doses (-41 and -56% for CCK 1 µg/kg and 3 µg/kg, respectively, $P<0.01$ compared to saline). After 20 min, CCK injection had no further effect on caloric intake in chow-fed rats (Fig. 3B). As expected, HF/HS diet-fed rats displayed decreased calorie intake during the first 20 min following the highest dose of CCK (-56%, $P<0.05$ compared to saline) but were

insensitive to the low dose (Fig. 3A and B). Surprisingly, LF diet-fed rats ate less calories than chow-fed rats under the saline condition (-41%, P=0.01 compared to chow-fed rats under saline). LF diet-fed rats administered either dose of CCK did not significantly decrease calorie intake during the first 20 minutes. This absence of effect of CCK on caloric intake in HF/HS-fed rats and LF-fed rats was not due to a delayed action of CCK since no effect of CCK was observed on caloric intake between 20 and 60 minutes in these animals (Fig. 3C and D).

Addition of inulin to the LF or HF/HS- diets had no significant effect on CCK-induced inhibition of food intake during the first 20 minutes (Fig. 3A and B). LF-I diet fed rats did not respond to either dose of CCK. Moreover, administration of CCK 3µg/kg significantly inhibited 20-min caloric intake by 58% (P<0.01 compared to saline) in HF/HS-I fed rats, but there was no response to the lower dose of CCK. (Fig. 3A and B). This difference in response to CCK compared to chow-fed animals was not due to a delayed effect of CCK since the 20-60 min caloric intake was not affected by CCK injection in LF-I or HF/HS-I diet fed rats (Fig. 3C and D).

We investigated whether rats fed the refined diets were sensitive to leptin by injecting rats with leptin or saline 2hrs before euthanasia. The level of PTP1b in the nodose ganglia evaluated by western blot was used as a marker of leptin downstream signaling. Due to technical problems, the nodose ganglia of only 2 chow-fed rats injected with leptin were analyzed, thus the following observations will be interesting to validate in future studies. The level of PTP1b after leptin injection increased compared to saline in chow-fed rats (Table 5). Conversely, leptin injection did not change PTP1b level in the nodose ganglia of LF-, LF-I and HF/HS-diet fed rats (Table 5) while it decreased PTP1b level in the nodose ganglia of HF/HS-I diet-fed rats (P=0.01, Table 5). These preliminary data suggest that rats fed the refined diets have altered leptin signaling in VAN compared to chow-fed ones.

Decrease in sensitivity to CCK correlated with adiposity parameters and plasma LBP

The most discriminant parameter between rats fed chow or the refined diets was the response to low dose CCK, which was blunted in refined diet-fed rats. Yet, a large variability in this parameter was observed between rats, even within a dietary group. We decided to take advantage of this variability to investigate if this parameter correlated with any phenotypic or metabolomic data (coefficient correlation in Suppl. Table 1).

The amount of calorie ingested during 20 min after CCK 1µg/kg injection correlated significantly and positively with several indexes of adiposity: adiposity index (Fig. 4A), mesenteric fat relative weight, retroperitoneal fat relative weight (Fig. 4B), epididymal fat relative weight (Fig. 4C), retroperitoneal fat adipocyte average size and frequency of large adipocytes in retroperitoneal fat (Fig. 4D). It also correlated positively with the caecal content levels of alanine and ethanol and negatively with that of 4-HPPA (Suppl. Table 1).

Because caloric intake of LF- and LF-I diet-fed rats was lower than that of the other groups even under saline, we also tested the change in calorie intake after CCK 1µg/kg injection compared to saline injection as an index of CCK sensitivity. Similarly, we found that this parameter correlated with adiposity index and the retroperitoneal fat pad relative weight (Fig. 4E). The decrease in calorie intake correlated significantly with plasma LBP (Fig. 4F). It also correlated significantly with the caecal content level of aspartate, one bile acid and one unknown compound (Suppl. Table 1).

DISCUSSION

Recent data have shown gut microbiota dysbiosis in rodents fed a refined LF diet and there is increasing evidence showing a link between gut dysbiosis and alteration in the CCK-leptin-VAN signaling pathway controlling satiation. We hypothesized that LF diets impair CCK-induced inhibition of food intake and that inulin could prevent this effect. We confirmed that LF diet consumption for 8 weeks impacted caecal metabolome compared to chow, suggesting altered microbiota function similar to that induced by a HF/HS diet. We also showed that LF diet consumption resulted in the loss of CCK satiation similar to that observed with HF/HS diet. Substituting inulin, a soluble fiber, for cellulose, an insoluble fiber, in refined diets minimally impacted the phenotype but prevented caecal atrophy and alteration of gut defense, and modulated the caecal metabolome. Interestingly, addition of inulin to either diet had no effect on CCK-induced inhibition of food intake. Taken together, these data suggest that although addition of a soluble fiber to synthetic diets may improve some aspects of gut microbial dysbiosis and host gut function, soluble fiber does not restore gut-brain signaling, specifically activation of vagal afferents by CCK.

Recent data suggest that the type of control diet (LF or chow) used in DIO studies can profoundly change the conclusion drawn from the studies since consumption of LF refined diets has been shown to alter host physiology and metabolism [21]. Our study is the first to investigate the effects of refined diet feeding on CCK induced inhibition of food intake. Low dose CCK injection did not induce a reduction in food intake in rats fed the refined diets, either LF or HF/HS, suggesting that similar to HF/HS-diet fed rats, LF-diet fed rats had reduced sensitivity to CCK compared to chow-fed rats. One caveat to this interpretation is that food intake was reduced significantly in LF diet-fed compared to chow-fed rats even after vehicle administration. Although there was no further inhibition of food intake with administration of CCK, it is possible that food intake had reached a “floor effect” where it was not possible to further reduce food intake in fasted rats. The reason for the decreased food intake under saline

411 as well as the decreased cumulative energy intake over the 8-week feeding period in LF-diet
412 fed rats is unknown. Feed conversion ratio, i.e. the calorie needed to gain weight was reduced
413 in LF- diet fed rats compared to chow-fed ones. This suggests that LF diet-fed rats extracted
414 enough energy and nutrients from the LF diet to sustain growth rate similar to that of chow.
415 The presence of purified ingredients in the refined diet probably accounts for this lower feed
416 conversion ratio. Similar results, i.e. decreased energy intake and lower feed conversion ratio
417 in LF-diet fed rats compared to chow-fed ones were observed by Sen et al. [12].
418
419 CCK sensitivity, expressed as calories ingested after injection of the low dose of CCK or as
420 the decrease in calorie intake after low dose of CCK injection, compared to saline injection,
421 correlated significantly to adiposity parameters. Despite similar growth rate, LF diet-fed rats
422 exhibited a trend for increase in adiposity index compared to chow-fed rats. The shape of their
423 adipocyte size distribution curve was shifted towards larger adipocytes compared to chow-fed
424 rats, suggesting accumulation of lipids in adipose tissue. Small, yet significant, increase in fat
425 pad weight has also been observed in mice or rats fed a refined LF diet compared to chow in
426 previous studies [9, 12, 21, 22]. Several studies reported muscle insulin resistance of mice or
427 rats fed a LF diet even early after the start of LF diet consumption [21, 22], leading to pancreas
428 compensation and high level of circulating insulin. In these studies though, LF diets contained
429 high levels of sucrose which could explain these metabolic perturbations. Our LF diet did not
430 contain sucrose. Thus the slight increase in adiposity in LF diet-fed rats which correlate
431 significantly with CCK sensitivity, would need further investigation.
432
433 We hypothesized that the lack of activation of VAN by CCK in refined diet-fed rats was a result
434 of leptin resistance. Several reports indicate that leptin resistance can be induced in relatively
435 short periods at normal body fat and leptin levels [23]. Our attempt to investigate leptin
436 signaling *via* the downstream mediator of leptin PTP1b in the nodose ganglia raised preliminary
437 but encouraging results suggesting impaired leptin signaling. However, this needs to be
438 confirmed. Another hypothesis is that the sucrose level in the diets could explain the lower

sensitivity to CCK in our refined-diet fed rats as demonstrated by Sen et al. [12]. However, our LF-diet did not contain sucrose. We therefore hypothesized that dysbiosis-induced translocation of LPS triggers impairment of leptin signaling and sensitivity to CCK in VAN as already demonstrated [14, 15]. *In vitro*, infusion of LPS on VAN primary culture increased suppressor of cytokine signaling 3 (SOCS3) expression, a marker of leptin resistance, in a dose-dependent manner [14]. Similarly, rats implanted with osmotic mini-pumps that chronically deliver LPS for 6 weeks exhibited increased SOCS3 expression in VAN, associated to decreased phosphorylation of signal transducers and activators of transcription 3, another marker of leptin signaling disruption [15]. HF/HS chronic consumption has been shown to induce dysbiosis and alter the intestinal and hepatic mechanisms involved in protection against LPS entry into the organisms, resulting in greater plasma LPS in HF/HS diet fed rats [24]. The impact of LF diet consumption on intestinal barrier function has not been evaluated so far. In the current study, we evaluated plasma LBP level and IAP activity, a major enzyme involved in defense mechanisms, especially against LPS [13] and can be induced by LPS itself [25]. The increased IAP activity observed in LF diet-fed compared to chow-fed rats could be a host adaptive response to altered microbiota composition and increased abundance of LPS-bearing bacteria as observed in DIO rats[24]. LBP is an acute-phase protein synthesized by hepatocytes in response to LPS and released into the bloodstream. As such plasma LBP is a useful marker of exposition to LPS [13]. Plasma LBP was not significantly different between chow- and refined-diet fed rats but was greater in LF-I diet-fed rats compared to LF diet-fed ones. Moreover, a significant positive correlation between calorie intake under CCK 1µg/kg and plasma LBP level was observed. Thus increased translocation of LPS in refined diet-fed rats might have disturbed signaling in VAN.

We show a significant difference in the caecal metabolomic profiles of C- *vs.* refined diet-fed rats, including LF-diet fed rats. Metabolic profiling has emerged as a valuable tool to evaluate modulation of gut microbiota metabolism in response to physiological or pathological changes. It can also serve as a fingerprint of biochemical perturbations unique to the nature or

mechanism of a particular biological process [26]. By analyzing the caecal metabolome using ^{1}H-NMR we were able to evaluate the consequences of LF-diet consumption on the levels of molecules directly in contact with the host. LF diet-fed rats exhibited lower caecal levels of several nucleic acids (hypoxanthine and a tendency for uracil). Similar decrease in uracil and hypoxanthine levels has been reported in the feces of DSS-induced colitic mice compared to healthy ones [27]. LF diet-fed rats also exhibited increased caecal levels of amino acids (isoleucine, lysine, phenylalanine, valine) with a concomitant decrease in the level of α-keto-isovalerate and the same tendency for 4-HPPA, two microbial products of amino acid metabolism. The level of short chain fatty acids (SCFA) acetate and propionate also tended to be lower in the caecum of LF diet- compared to chow-fed rats, although not significant. Similar metabolomics profiles with increased levels of amino acids and decreased levels of short chain fatty acids have been reported in the feces of ulcerative colitis patients [28]. The similarity between the intestinal metabolome of our LF diet-fed rats and of animal models and humans with an inflamed gut suggests intestinal inflammation after LF diet consumption. Inflammation occurring with a LF diet has also been observed in the adipose tissue of mice which exhibited greater MCP-1 mRNA levels compared to chow-fed mice [21]. This suggests that refined LF diet can promote inflammation, either intestinal or systemic. It is possible that some of the effects of refined diets might be dependent on the lack of soluble fiber [9].

We chose to investigate how the substitution of inulin for cellulose in our refined diets affected CCK signaling given that inulin has been previously shown to prevent gut microbiota alteration and gut atrophy, and these parameters have been linked to CCK signaling. Dietary inulin did not modify weight gain and adiposity in HF/HS-I diet -fed rats. Only a slight improvement in the adipocyte size distribution was observed. Many publications have shown the beneficial effects of adding soluble fiber to purified diets to improve health in rodent models. In the context of purified ingredient diets, the addition of soluble fiber like inulin, fructo-oligosaccharides, and pectin improves gut morphology and reduce body weight and adiposity relative to insoluble cellulose[29–36]. However, some studies also reported poor effect of inulin or inulin-

oligofructose mix on weight gain and adiposity [9, 37, 38]. Specifically, Zou et al. showed that inulin added to a HF/HS diet did not decrease weight gain compared to the same amount of cellulose added to a HF/HS diet [36]. Moreover, recent data demonstrated worsening of intestinal inflammation with inulin or fructo-oligosaccharides in refined diet-fed mice colitis models [39, 40], suggesting that the effect of fermentable fiber in refined diet is not as clear. Difference in dose, type of inulin, time of dietary intervention but also the type/cause of inflammatory condition probably explain the discrepancies between studies.

Despite the absence of effect of inulin on adiposity in our model, dietary inulin clearly prevented caecal atrophy and the increased in IAP activity. It also significantly changed the caecal metabolomic profiles by preventing the changes in the caecal level of several metabolites (isoleucine, valine, α-keto-isovalerate, hypoxanthine, uracil) and by increasing butyrate caecal level in LF-I diet-fed rats. Yet, inulin also increased the caecal level of several other amino acids, especially in LF-I diet-fed animals (alanine, aspartate, tyrosine and glutamate) and enhanced some changes already observed with LF and HF/HS diets, further increasing the concentration of phenylalanine and decreasing that of 4-HPPA in the caecal lumen of rats. Inulin supplementation has previously been associated with increased mucin secretion in the caecal lumen in rats fed refined diets [41] and increased abundance of proteolytic bacteria including *Enterococcus* and bacteria belonging to the genus *Clostridium* [42]. Concomitant elevated mucus secretion and proteolytic activities could explain the elevated amino acid levels in the caecal lumen of inulin fed rats. Furthermore, fermentation of amino acids by bacteria is decreased at low pH compared to neutral pH [43]. Relative to cellulose, adding inulin to a diet decreases caecal pH [41, 44] and might therefore reduce amino acid bacterial utilization, consistent with the decreased level of amino acid metabolism end-products 4-HPPA and α-keto-isovalerate. Besides modulating pH, inulin supplementation has also been associated with modulation of SCFA bacterial production despite conflicting results in the literature. In our model, dietary inulin only slightly changed SCFA levels in the caecum, with only a modest increase in butyrate level in LF-I diet-fed animals. In mice, one study reported that inulin

supplementation increased acetate production but did not modify butyrate and propionate caecal levels [9]. In humans, two studies showed decreased SCFA concentrations during inulin supplementation [45, 46]. Despite no effects of inulin on SCFA level in our model, inulin supplementation prevented caecal tissue atrophy as previously observed [9, 41, 44]. We speculate that inulin enhanced gut microbiota SCFA production and subsequent absorption of SCFA by the colonocytes, preventing their detection in the caecal metabolome of inulin-fed rats but resulting in colonocytes proliferation and caecal weight maintenance. Finally, although inulin added to refined diets improved caecal homeostasis, metabolomics data indicate that the gut microbiota of inulin-fed rats is still different from that of chow-fed rats, suggesting that host-microbiota interactions in these inulin-fed animals are probably still different from that of chow-fed rats.

In conclusion, our study provides evidence that refined LF diet consumption for 8 weeks reduced rat CCK sensitivity and profoundly impacted caecal metabolome which was similar to that of HF/HS-diet fed rats. Inulin prevented caecal atrophy and prevented some, but not all, of the metabolomic alterations induced by refined diet consumption. Overall, our data highlight the fact that even if chow is not the preferred control diet in terms of dietary constituents, it must be included as a proper control of microbiota-host homeostasis and normal rodent development defined by years of previous research. Caution must be taken when using LF diet which profoundly alters the equilibrium in the gut until a more suitable refined control diet is identified.

Acknowledgments

The authors would like to thank Cécile Canlet from the French National Infrastructure of Metabolomics and Fluxomics (MetaboHUB-ANR-11-INBS-0010) for her help with the NMR facility and Dr. Olivier Cloarec from Korrigan Sciences Limited for providing the matlab functions for analysis of NMR data. They also want to thank Ricky Stephens for his help in animal experiment.

551 MG, MKH, CCR, HER and GB designed research, MG, MKH, CCR, SES conducted research,
552 MG, SES analyzed data, MG, MKH, SES, HER and GB wrote the paper. GB had primarily
553 responsibility for final content. All authors read and approved final version.
554 The authors have no conflict of interest to declare.

References

1. Dockray GJ (2014) Gastrointestinal hormones and the dialogue between gut and brain: Gut-brain signalling. J Physiol 592:2927–2941 . doi: 10.1113/jphysiol.2014.270850

2. Raybould HE (2007) Mechanisms of CCK signaling from gut to brain. Curr Opin Pharmacol 7:570–574 . doi: 10.1016/j.coph.2007.09.006

3. de Lartigue G, Dimaline R, Varro A, Dockray GJ (2007) Cocaine- and Amphetamine-Regulated Transcript: Stimulation of Expression in Rat Vagal Afferent Neurons by Cholecystokinin and Suppression by Ghrelin. J Neurosci 27:2876–2882 . doi: 10.1523/JNEUROSCI.5508-06.2007

4. Campos CA, Wright JS, Czaja K, Ritter RC (2012) CCK-induced reduction of food intake and hindbrain MAPK signaling are mediated by NMDA receptor activation. Endocrinology 153:2633–2646 . doi: 10.1210/en.2012-1025

5. de Lartigue G, Barbier de la Serre C, Espero E, et al (2012) Leptin Resistance in Vagal Afferent Neurons Inhibits Cholecystokinin Signaling and Satiation in Diet Induced Obese Rats. PLoS ONE 7:e32967 . doi: 10.1371/journal.pone.0032967

6. Duca FA, Zhong L, Covasa M (2013) Reduced CCK signaling in obese-prone rats fed a high fat diet. Horm Behav 64:812–817 . doi: 10.1016/j.yhbeh.2013.09.004

7. Warden CH, Fisler JS (2008) Comparisons of Diets Used in Animal Models of High-Fat Feeding. Cell Metab 7:277 . doi: 10.1016/j.cmet.2008.03.014

8. Pellizzon MA, Ricci MR (2018) The common use of improper control diets in diet-induced metabolic disease research confounds data interpretation: the fiber factor. Nutr Metab 15: . doi: 10.1186/s12986-018-0243-5

9. Chassaing B, Miles-Brown J, Pellizzon M, et al (2015) Lack of soluble fiber drives diet-induced adiposity in mice. Am J Physiol-Gastrointest Liver Physiol 309:G528–G541 . doi: 10.1152/ajpgi.00172.2015

10. Dalby MJ, Ross AW, Walker AW, Morgan PJ (2017) Dietary Uncoupling of Gut Microbiota and Energy Harvesting from Obesity and Glucose Tolerance in Mice. Cell Rep 21:1521–1533 . doi: 10.1016/j.celrep.2017.10.056

11. Vaughn AC, Cooper EM, DiLorenzo PM, et al (2017) Energy-dense diet triggers changes in gut microbiota, reorganization of gut‐brain vagal communication and increases body fat accumulation. Acta Neurobiol Exp (Warsz) 77:18–30

12. Sen T, Cawthon CR, Ihde BT, et al (2017) Diet-driven microbiota dysbiosis is associated with vagal remodeling and obesity. Physiol Behav 173:305–317 . doi: 10.1016/j.physbeh.2017.02.027

13. Guerville M, Boudry G (2016) Gastrointestinal and hepatic mechanisms limiting entry and dissemination of lipopolysaccharide into the systemic circulation. Am J Physiol-Gastrointest Liver Physiol 311:G1–G15 . doi: 10.1152/ajpgi.00098.2016

14. de Lartigue G, Barbier de la Serre C, Espero E, et al (2011) Diet-induced obesity leads to the development of leptin resistance in vagal afferent neurons. Am J Physiol-Endocrinol Metab 301:E187–E195 . doi: 10.1152/ajpendo.00056.2011

15. de La Serre CB, de Lartigue G, Raybould HE (2015) Chronic exposure to Low dose bacterial lipopolysaccharide inhibits leptin signaling in vagal afferent neurons. Physiol Behav 139:188–194 . doi: 10.1016/j.physbeh.2014.10.032

16. Cawthon CR, de La Serre CB (2018) Gut bacteria interaction with vagal afferents. Brain Res. doi: 10.1016/j.brainres.2018.01.012

17. Dieterle F, Ross A, Schlotterbeck G, Senn H (2006) Metabolite Projection Analysis for Fast Identification of Metabolites in Metabonomics. Application in an Amiodarone Study. Anal Chem 78:3551–3561 . doi: 10.1021/ac0518351

18. Veselkov KA, Lindon JC, Ebbels TMD, et al (2009) Recursive Segment-Wise Peak Alignment of Biological ^{1}H NMR Spectra for Improved Metabolic Biomarker Recovery. Anal Chem 81:56–66 . doi: 10.1021/ac8011544

19. Cloarec O, Dumas ME, Trygg J, et al (2005) Evaluation of the Orthogonal Projection on Latent Structure Model Limitations Caused by Chemical Shift Variability and Improved Visualization of Biomarker Changes in ^{1}H NMR Spectroscopic Metabonomic Studies. Anal Chem 77:517–526 . doi: 10.1021/ac048803i

20. Estaki M, DeCoffe D, Gibson DL (2014) Interplay between intestinal alkaline phosphatase, diet, gut microbes and immunity. World J Gastroenterol 20:15650–15656 . doi: 10.3748/wjg.v20.i42.15650

21. Benoit B, Plaisancié P, Awada M, et al (2013) High-fat diet action on adiposity, inflammation, and insulin sensitivity depends on the control low-fat diet. Nutr Res 33:952–960 . doi: 10.1016/j.nutres.2013.07.017

22. Apolzan JW, Harris RBS (2012) Differential effects of chow and purified diet on the consumption of sucrose solution and lard and the development of obesity. Physiol Behav 105:325–331 . doi: 10.1016/j.physbeh.2011.08.023

23. Vasselli JR, Scarpace PJ, Harris RBS, Banks WA (2013) Dietary components in the development of leptin resistance. Adv Nutr Bethesda Md 4:164–175 . doi: 10.3945/an.112.003152

24. Guerville M, Leroy A, Sinquin A, et al (2017) Western-diet consumption induces alteration of barrier function mechanisms in the ileum that correlates with metabolic endotoxemia in rats. Am J Physiol-Endocrinol Metab 313:E107–E120 . doi: 10.1152/ajpendo.00372.2016

25. Lallès J-P (2014) Intestinal alkaline phosphatase: novel functions and protective effects. Nutr Rev 72:82–94 . doi: 10.1111/nure.12082

26. Storr M, Vogel HJ, Schicho R (2013) Metabolomics: is it useful for inflammatory bowel diseases? Curr Opin Gastroenterol 29:378–383 . doi: 10.1097/MOG.0b013e328361f488

27. Hong Y-S, Ahn Y-T, Park J-C, et al (2010) 1H NMR-based metabonomic assessment of probiotic effects in a colitis mouse model. Arch Pharm Res 33:1091–1101 . doi: 10.1007/s12272-010-0716-1

28. Bjerrum JT, Wang Y, Hao F, et al (2015) Metabonomics of human fecal extracts characterize ulcerative colitis, Crohn's disease and healthy individuals. Metabolomics 11:122–133 . doi: 10.1007/s11306-014-0677-3

29. Adam CL, Williams PA, Dalby MJ, et al (2014) Different types of soluble fermentable dietary fibre decrease food intake, body weight gain and adiposity in young adult male rats. Nutr Metab 11:36 . doi: 10.1186/1743-7075-11-36

30. Adam CL, Williams PA, Garden KE, et al (2015) Dose-Dependent Effects of a Soluble Dietary Fibre (Pectin) on Food Intake, Adiposity, Gut Hypertrophy and Gut Satiety Hormone Secretion in Rats. PLOS ONE 10:e0115438 . doi: 10.1371/journal.pone.0115438

31. Levrat M-A, Rémésy C, Demigné C (1991) High Propionic Acid Fermentations and Mineral Accumulation in the Cecum of Rats Adapted to Different Levels of Inulin. J Nutr 121:1730–1737 . doi: 10.1093/jn/121.11.1730

32. Respondek F, Gerard P, Bossis M, et al (2013) Short-Chain Fructo-Oligosaccharides Modulate Intestinal Microbiota and Metabolic Parameters of Humanized Gnotobiotic Diet Induced Obesity Mice. PLoS ONE 8:e71026 . doi: 10.1371/journal.pone.0071026

33. Neyrinck AM, Van Hée VF, Piront N, et al (2012) Wheat-derived arabinoxylan oligosaccharides with prebiotic effect increase satietogenic gut peptides and reduce metabolic endotoxemia in diet-induced obese mice. Nutr Diabetes 2:e28–e28 . doi: 10.1038/nutd.2011.24

34. Nicolucci AC, Hume MP, Martínez I, et al (2017) Prebiotics Reduce Body Fat and Alter Intestinal Microbiota in Children Who Are Overweight or With Obesity. Gastroenterology 153:711–722 . doi: 10.1053/j.gastro.2017.05.055

35. Brooks L, Viardot A, Tsakmaki A, et al (2017) Fermentable carbohydrate stimulates FFAR2-dependent colonic PYY cell expansion to increase satiety. Mol Metab 6:48–60 . doi: 10.1016/j.molmet.2016.10.011

36. Zou J, Chassaing B, Singh V, et al (2018) Fiber-Mediated Nourishment of Gut Microbiota Protects against Diet-Induced Obesity by Restoring IL-22-Mediated Colonic Health. Cell Host Microbe 23:41-53.e4 . doi: 10.1016/j.chom.2017.11.003

37. Dewulf EM, Cani PD, Claus SP, et al (2013) Insight into the prebiotic concept: lessons from an exploratory, double blind intervention study with inulin-type fructans in obese women. Gut 62:1112–1121 . doi: 10.1136/gutjnl-2012-303304

38. Hamilton MK, Ronveaux CC, Rust BM, et al (2017) Prebiotic milk oligosaccharides prevent development of obese phenotype, impairment of gut permeability, and microbial dysbiosis in high fat-fed mice. Am J Physiol-Gastrointest Liver Physiol 312:G474–G487 . doi: 10.1152/ajpgi.00427.2016

39. Goto H, Takemura N, Ogasawara T, et al (2010) Effects of Fructo-Oligosaccharide on DSS-Induced Colitis Differ in Mice Fed Nonpurified and Purified Diets1,2. J Nutr 140:2121–2127 . doi: 10.3945/jn.110.125948

40. Miles JP, Zou J, Kumar M-V, et al (2017) Supplementation of Low- and High-fat Diets with Fermentable Fiber Exacerbates Severity of DSS-induced Acute Colitis: Inflamm Bowel Dis 23:1133–1143 . doi: 10.1097/MIB.0000000000001155

41. Van den Abbeele P, Gérard P, Rabot S, et al (2011) Arabinoxylans and inulin differentially modulate the mucosal and luminal gut microbiota and mucin-degradation in humanized rats: Prebiotics modulate mucosal and luminal microbiota summary. Environ Microbiol 13:2667–2680 . doi: 10.1111/j.1462-2920.2011.02533.x

42. Cani PD, Possemiers S, Van de Wiele T, et al (2009) Changes in gut microbiota control inflammation in obese mice through a mechanism involving GLP-2-driven improvement of gut permeability. Gut 58:1091–1103 . doi: 10.1136/gut.2008.165886

43. Dai Z-L, Wu G, Zhu W-Y (2011) Amino acid metabolism in intestinal bacteria: links between gut ecology and host health. Front Biosci Landmark Ed 16:1768–1786

44. Juśkiewicz J, Zduńczyk Z (2004) Effects of cellulose, carboxymethylcellulose and inulin fed to rats as single supplements or in combinations on their caecal parameters. Comp Biochem Physiol A Mol Integr Physiol 139:513–519 . doi: 10.1016/j.cbpb.2004.10.015

45. Salazar N, Dewulf EM, Neyrinck AM, et al (2015) Inulin-type fructans modulate intestinal Bifidobacterium species populations and decrease fecal short-chain fatty acids in obese women. Clin Nutr 34:501–507 . doi: 10.1016/j.clnu.2014.06.001

46. Teixeira TFS, Grześkowiak Ł, Franceschini SCC, et al (2013) Higher level of faecal SCFA in women correlates with metabolic syndrome risk factors. Br J Nutr 109:914–919 . doi: 10.1017/S0007114512002723

Supporting information:

S1 Fig 1. Assigned 600 MHz 1D NMR spectra of mouse caecal content. The 5 to 9 ppm region was vertically expended 6 times compared to the 0 to 4.5 ppm region. Keys: 1: bile acids (mixed), 2: butyrate, 3: leucine, 4: isoleucine, 5: valine, 6: propionate, 7: α-ketoisovalerate, 8: ethanol, 9: β-hydroxybutyrate, 10: lipids, 11: lactate, 12: alanine, 13: lysine, 14: acetate, 15: N-acetyl groups, 16: glutamate, 17: succinate, 18: α-ketoglutarate, 19: aspartate, 20: choline, 21: taurine, 22: β-xylose, 23: β-galactose, 24: β-glucose, 25: α-arabinose, 26: α-xylose, 27: α-glucose, 28: α-galactose, 29: uracil, 30: tyrosine, 31: phenylalanine, 32: adenine, 33: hypoxanthine, 34: formate.

S2 Table 1. Correlation coefficients

Figures legend

Figure 1: Effect of diets on rat phenotype.

Percent body weight gain (A), weight gain (B), average daily energy intake (C), cumulative food intake (D), feed conversion ratio (E) over the 8-week period, plasma LPS-binding protein (F), adiposity index (G) and distribution of adipocyte size in retroperitoneal fat pads (H) after 8 week of Chow (black), LF (grey), LF-I (striped grey), HF/HS (white) and HF/HS-I (dotted white) -diet consumption.

Data are expressed as mean ± SEM, (n=8 rats per group, except LBP n=5 to 8 and adipocyte size n=4). Means with different letters are significantly different (P<0.05). * P<0.05 HF- *vs.* chow-diet, $ P<0.05 HF-I *vs.* chow-diet.

Figure 2: Effect of diets on caecal metabolome, morphology and IAP activity.

O-PLS-DA cross-validated score plots showing the discrimination between ^{1}H-NMR spectra of caecal contents from rats fed Chow vs refined LF vs HF/HS diets (A), HF/HS vs LF (B), Chow vs refined diet LF vs LF-I diets (E), Chow vs HF/HS vs HF/HS-I diets (F) and LF vs LF-I vs HF/HS vs HF/HS-I diets (G).

O-PLS-DA correlation loading plots relative to the discrimination between ^{1}H-NMR spectra of caecal contents from rats fed Chow vs LF (C) or Chow vs. HF/HS (D) or LF vs LF-I (H) diets. Metabolites are color-coded according their correlation coefficient, red indicating a very strong positive correlation. The direction of the metabolite indicates the group with which it is positively associated as labeled on the diagrams. BCAA: branched-chain amino acids, hpx: hypoxanthine, 4-HPPA: 4-hydroxyphenylacetate, uk: unknown compound.

Caecum tissue relative weight (I) and caecal IAP activity (J) in Chow, LF, LF-I, HF/HS and HF/HS-I–diet fed rats at week 8. Values are means ± SEM (n=8 rats per group). Means with different letters are significantly different (P<0.05).

Figure 3: Effect of diets on CCK satiation

Intake expressed as actual energy intake (A, C) or as percentage of saline energy intake after 20 min (A, B) or from 20 to 60 min (C, D) after intraperitoneal injection of either saline (400 µl) or CCK-8S at the lowest dose (1µg/kg body weight) or the highest dose (3 µg/kg of body weight) of Chow (black), LF (grey), LF-I (striped grey), HF/HS (white) and HF/HS-I (dotted white) diet-fed rats.

Values are means ± SEM (n=7 to 8 rats per group). Each rat received vehicle and the two CCK doses randomly. * $P<0.05$ compared to saline in the same dietary group.

Figure 4: Correlations between calorie intake after CCK low dose injection and adiposity parameters.

Correlation between energy intake after CCK 1µg/kg and adiposity index (A), retroperitoneal fat pad relative weight (B), epididymal fat pad relative weight (C), percentage of large adipocytes in the retroperitoneal fat pad (D) and between decrease in energy intake after CCK 1µg/kg expressed in percent of intake under saline and retroperitoneal fat pad relative weight (E) or plasma LBP (F). Each point represents one animal: black circle: chow, grey square: LF, open square: LF-I, black triangle: HF/HS, open triangle: HF/HS-I.

Figure 1

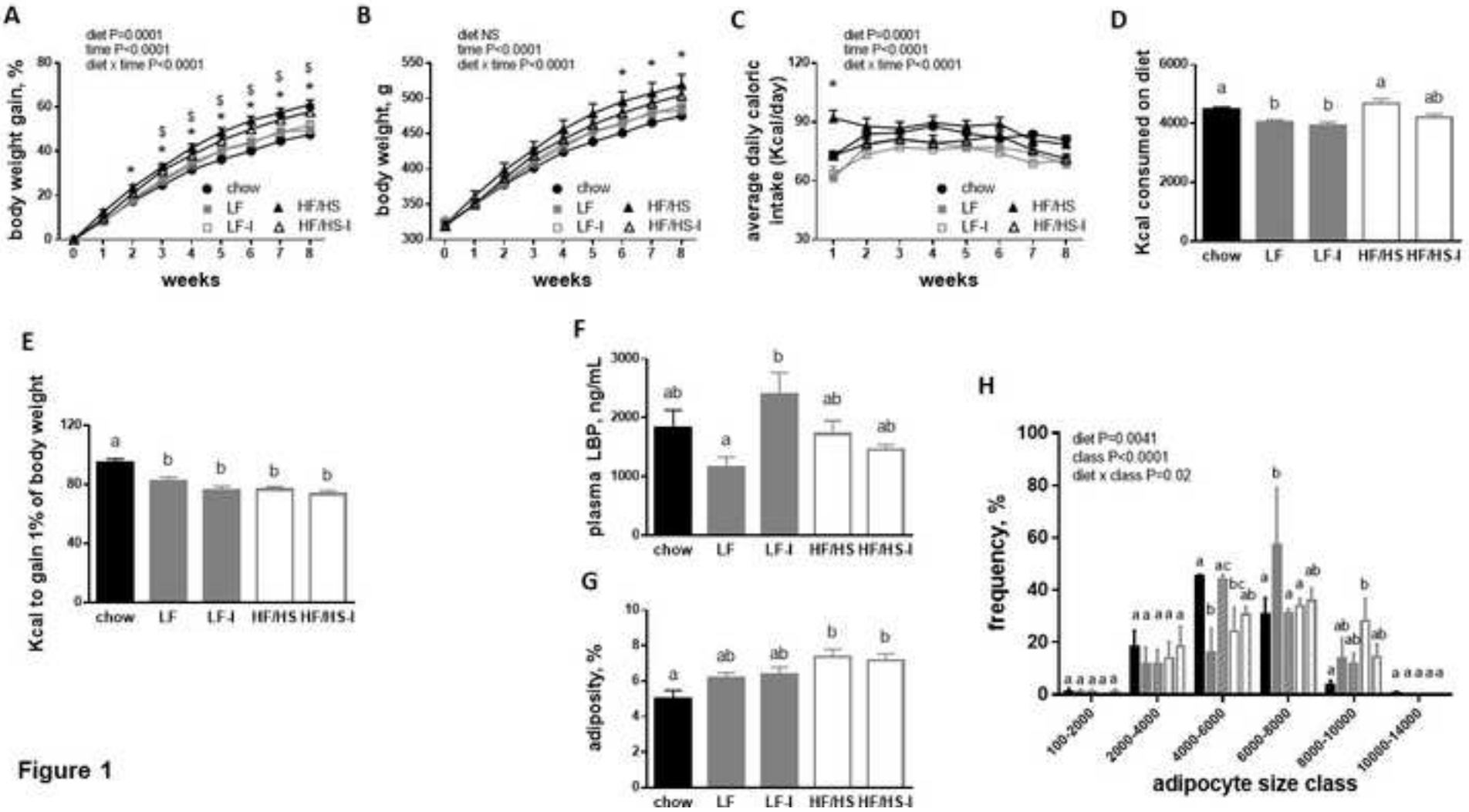

Figure 1

Figure 2

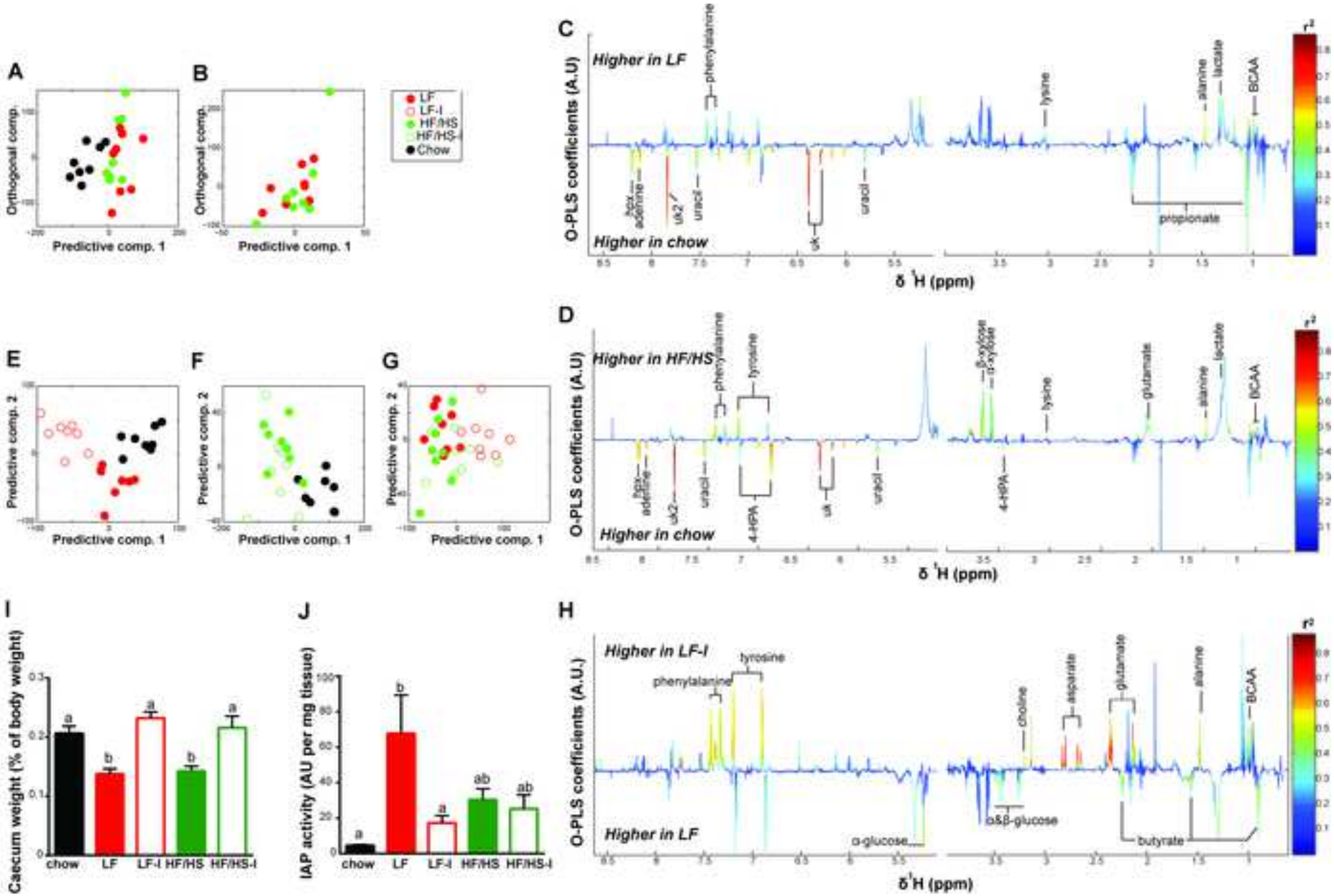

Figure 3

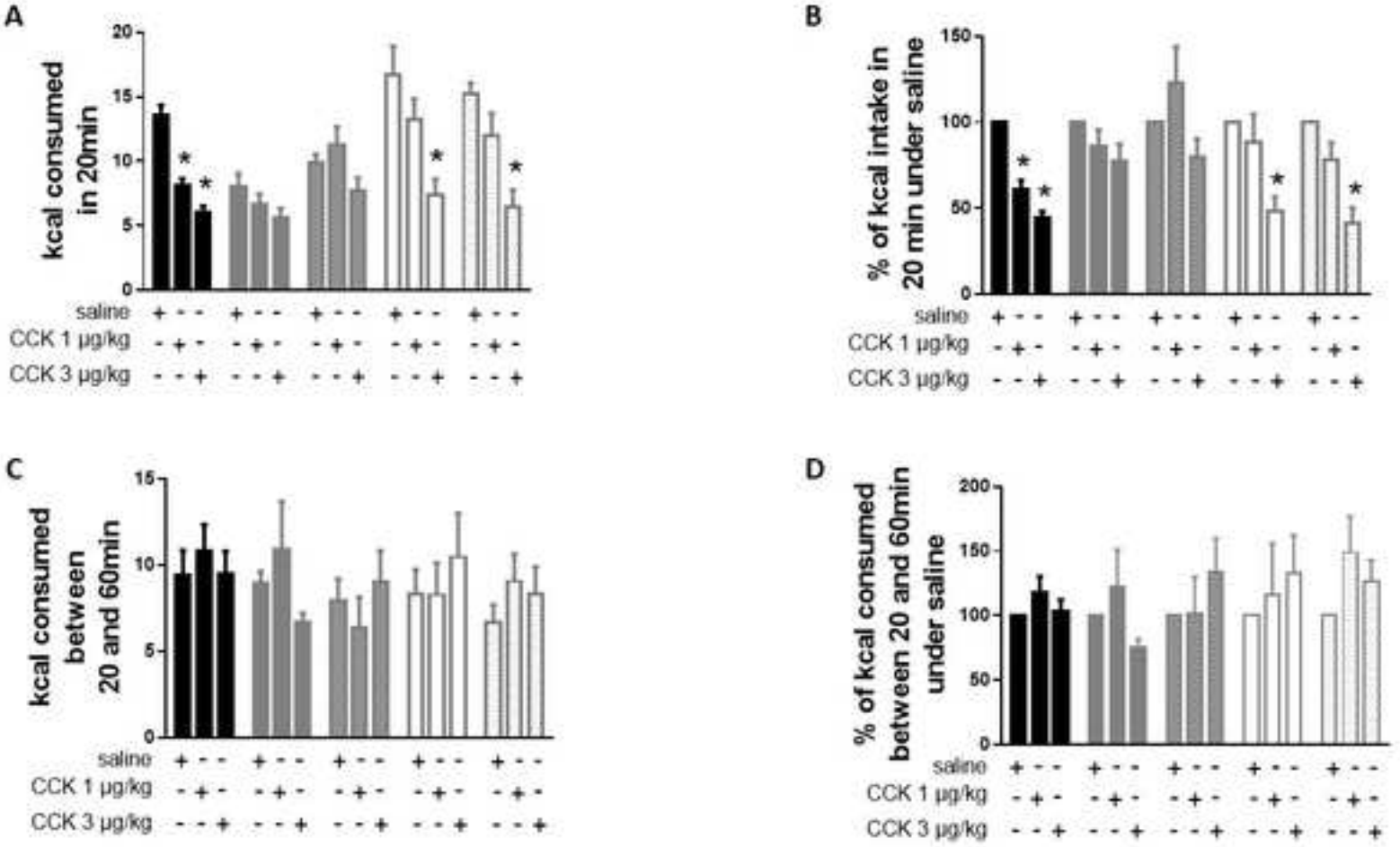

Figure 4

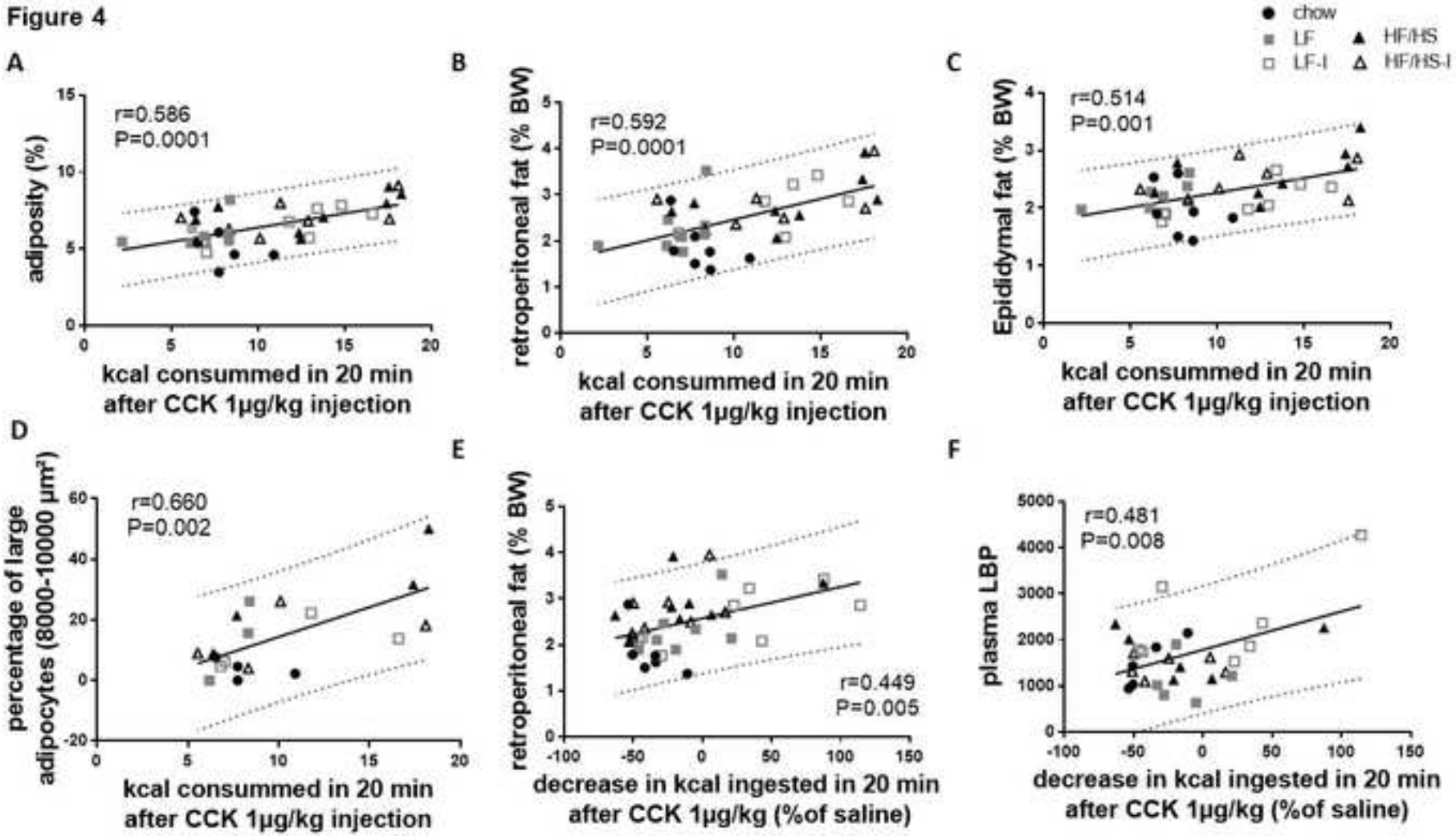

Table 1: Ingredient composition and macronutrient contribution to energy of the chow diet.

Ingredients :	
Ground corn, dehulled soybean meal, dried beet pulp, fish meal, ground oats, brewers dried yeast, cane molasses, dehydrated alfalfa meal, dried whey, wheat germ, porcine animal fat, porcine meat meal, wheat midlings, salt, vitamin mixture, mineral mixture	
Energy (%)	
Proteins	29
Lipids	13
Carbohydrates	58

Table 3: OPLS-DA model parameters and validation statistics calculated from ^{1}H NMR caecal content spectra.

Model	Number of predictive components	Number of orthogonal components	R^2X	R^2Y	Q^2Y	p-value[1]
Chow vs LF vs HF/HS	1	1	0.11	0.96	0.76	0.001
HF/HS vs LF	1	1	0.06	0.70	-0.08	0.52
Chow vs LF	1	1	0.13	0.97	0.67	0.001
Chow vs HF/HS	1	1	0.15	0.97	0.75	0.001
Chow vs LF vs LF-I	2	0	0.19	0.82	0.59	0.001
Chow vs HF/HS vs HF/HS-I	2	0	0.17	0.78	0.44	0.001
LF vs LF-I vs HF/HS vs HF/HS-I	2	1	0.11	0.86	0.34	0.001
HF vs HF/HS-I	1	0	0.07	0.76	0.08	0.26
LF vs LF-I	1	1	0.13	0.75	0.98	0.001

[1] Cumulative probability value determined at the 95th percentile to determine whether the result of the model was significantly different from the result calculated from 1000 random permutations of Y.

Table 3: OPLS-DA model parameters and validation statistics calculated from ^{1}H NMR caecal content spectra.

Model	Number of predictive components	Number of orthogonal components	R^2X	R^2Y	Q^2Y	p-value[1]
Chow vs LF vs HF/HS	1	1	0.11	0.96	0.76	0.001
HF/HS vs LF	1	1	0.06	0.70	-0.08	0.52
Chow vs LF	1	1	0.13	0.97	0.67	0.001
Chow vs HF/HS	1	1	0.15	0.97	0.75	0.001
Chow vs LF vs LF-I	2	0	0.19	0.82	0.59	0.001
Chow vs HF/HS vs HF/HS-I	2	0	0.17	0.78	0.44	0.001
LF vs LF-I vs HF/HS vs HF/HS-I	2	1	0.11	0.86	0.34	0.001
HF vs HF/HS-I	1	0	0.07	0.76	0.08	0.26
LF vs LF-I	1	1	0.13	0.75	0.98	0.001

[1] Cumulative probability value determined at the 95th percentile to determine whether the result of the model was significantly different from the result calculated from 1000 random permutations of Y.

Table 4. Changes in caecal content metabolites of rats fed LF, LF-I, HF/HS or HF/HS-I diets relative to chow diet (area under the curves of selected 1H-NMR peaks expressed as fold-change compared to chow).

Metabolites	Diagnostic NMR shift in ppm (multiplicity)	Chow	LF	LF-I	HF/HS	HF/HS-I	P-Value
Bile acid 1	0.66 (s)	1.00 ± 0.22	0.38 ± 0.10	0.74 ± 0.14	0.66 ± 0.21	1.31 ± 0.37	*0.07*
Bile acid 2	0.68 (s)	1.00 ± 0.22	0.73 ± 0.23	0.55 ± 0.11	0.79 ± 0.31	0.62 ± 0.13	*0.67*
Bile acid 3	0.7 (s)	1.00 ± 0.15	0.54 ± 0.09	0.63 ± 0.16	0.56 ± 0.20	0.74 ± 0.20	*0.30*
Bile acid 4	0.73 (s)	1.00 ± 0.20	1.05 ± 0.29	0.66 ± 0.18	0.62 ± 0.16	0.76 ± 0.18	*0.92*
Lactate	4.11 (q)	1.00 ± 0.07	0.96 ± 0.05	0.93 ± 0.07	0.98 ± 0.08	0.94 ± 0.08	*0.95*
Acetate	1.92 (s)	1.00 ± 0.10	0.74 ± 0.13	0.78 ± 0.12	0.74 ± 0.13	0.71 ± 0.11	*0.42*
Propionate	1.05 (t)	1.00 ± 0.07	0.71 ± 0.08	0.68 ± 0.13[,]	0.96 ± 0.14	0.64 ± 0.10	*0.06*
Butyrate	0.9 (t)	1.00 ± 0.07 [ab]	0.95 ± 0.22 [ab]	1.42 ± 0.32 [b]	0.57 ± 0.03 [a]	0.86 ± 0.08 [ab]	***0.03***

Alanine	1.48 (d)	1.00 ± 0.09 [a]	1.30 ± 0.10 [a]	1.97 ± 0.16 [b]	1.44 ± 0.19 [ab]	1.93 ± 0.10 [b]	***<0.0001***
Aspartate	2.38 (dd)	1.00 ± 0.07 [a]	1.32 ± 0.02 [a]	3.11 ± 0.25 [c]	1.67 ± 0.23 [ab]	2.17 ± 0.24 [b]	***<0.0001***
Glutamate	2.36 (m)	1.00 ± 0.07 [a]	1.00 ± 0.07 [a]	1.76 ± 0.14 [b]	1.01 ± 0.11 [a]	1.14 ± 0.20 [a]	***0.0003***
Isoleucine	1.01 (d)	1.00 ± 0.10 [a]	2.56 ± 0.24 [c]	1.77 ± 0.12 [b]	2.32 ± 0.27 [c]	1.54 ± 0.13 [b]	***<0.0001***
Leucine	0.96 (t)	1.00 ± 0.10	0.99 ± 0.14	0.71 ± 0.05	0.97 ± 0.16	0.77 ± 0.10	*0.26*
Lysine	3.03 (t)	1.00 ± 0.08 [a]	1.53 ± 0.21 [b]	1.65 ± 0.12 [b]	1.31 ± 0.09 [ab]	1.51 ± 0.07 [b]	***0.008***
Ornithine	1.7 (m)	1.00 ± 0.09	1.11 ± 0.11	1.28 ± 0.07	0.94 ± 0.09	1.15 ± 0.09	*0.08*
Phenylalanine	7.42 (t)	1.00 ± 0.12 [a]	1.39 ± 0.11 [ab]	2.10 ± 0.17 [b]	1.45 ± 0.06 [ab]	1.99 ± 0.16 [b]	***<0.0001***
Taurine	3.43 (t)	1.00 ± 0.29	1.19 ± 0.23	0.68 ± 0.12	1.20 ± 0.36	1.43 ± 0.31	*0.41*
Tyrosine	6.9 (t)	1.00 ± 0.12 [a]	1.23 ± 0.09 [ab]	1.99 ± 0.17 [b]	1.29 ± 0.06 [ab]	1.83 ± 0.18 [b]	***<0.0001***
Valine	0.99 (d)	1.00 ± 0.09 [a]	2.36 ± 0.36 [b]	1.38 ± 0.10 [ab]	1.75 ± 0.14 [ab]	1.29 ± 0.10 [ab]	***0.0001***
5-aminovalerate	2.24 (t)	1.00 ± 0.10 [ab]	1.48 ± 0.25 [b]	0.67 ± 0.12 [a]	1.08 ± 0.09 [ab]	1.14 ± 0.20 [ab]	***0.03***
α-keto-isovalerate	1.13 (d)	1.00 ± 0. 08 [a]	0.48 ± 0.09 [b]	0.64 ± 0.13 [ab]	0.65 ± 0.14 [ab]	0.64 ± 0.09 [ab]	***0.03***
4-HPPA	6.86 (d)	1.00 ± 0.12 [a]	0.62 ± 0.28 [a]	0.14 ± 0.03 [b]	0.32 ± 0.08 [ab]	0.14 ± 0.02 [b]	***<0.0001***
α-glucose	5.25 (d)	1.00 ± 0.13	1.54 ± 0.18	1.15 ± 0.15	1.56 ± 0.21	1.41 ± 0.21	*0.13*
β-glucose	4.65 (d)	1.00 ± 0.08 [ab]	1.31 ± 0.34 [b]	0.76 ± 0.07 [a]	0.93 ± 0.13 [ab]	1.11 ± 0.18 [ab]	***0.05***
succinate	2.4 (s)	1.00 ± 0.11	1.09 ± 0.39	1.26 ± 0.53	0.94 ± 0.22	1.95 ± 0.63	*0.45*

β-hydroxybutyrate	1.25 (d)	1.00 ± 0.14 [a]	1.80 ± 0.63 [ab]	1.44 ± 0.27 [ab]	2.88 ± 0.63 [b]	2.24 ± 0.49 [ab]	***0.03***
α-keto-glutarate	2.45 (t)	1.00 ± 0.10 [a]	0.69 ± 0.13 [ab]	0.52 ± 0.03 [ab]	0.60 ± 0.09 [ab]	0.43 ± 0.05 [b]	***0.03***
N-acetyl group	2.05 (s)	1.00 ± 0.14	1.32 ± 0.25	1.35 ± 0.16	1.68 ± 0.20	1.47 ± 0.21	*0.19*
Trimethylamine	2.9 (s)	1.00 ± 0.08 [a]	0.79 ± 0.07 [ab]	0.84 ± 0.07 [ab]	0.69 ± 0.08 [b]	0.71 ± 0.08 [ab]	***0.04***
Choline	3.2 (s)	1.00 ± 0.16 [ab]	0.81 ± 0.09 [a]	1.57 ± 0.22 [b]	0.84 ± 0.01 [a]	1.05 ± 0.12 [ab]	***0.005***
Uracil	5.8 (d)	1.00 ± 0.10	0.69 ± 0.08	0.85 ± 0.11	0.59 ± 0.11	0.66 ± 0.13	*0.07*
Hypoxanthine	8.19 (s)	1.00 ± 0.09 [a]	0.63 ± 0.06 [b]	0.76 ± 0.07 [ab]	0.50 ± 0.07 [b]	0.54 ± 0.08 [b]	***0.0003***
Unknown 1	6.38 (s)	1.00 ± 0.12 [a]	0.14 ± 0.02 [b]	0.13 ± 0.03 [b]	0.10 ± 0.01 [b]	0.14 ± 0.02 [b]	***<0.0002***
Unknown 2	6.70 (m)	1.00 ± 0.11	0.87 ± 0.40	0.61 ± 0.20	1.74 ± 0.88	0.85 ± 0.21	*0.47*
Unknown 4	6.38 (m)	1.00 ± 0.12 [a]	0.09 ± 0.01 [b]	0.09 ± 0.02 [b]	0.07 ± 0.01 [b]	0.09 ± 0.02 [b]	***<0.0001***
Ethanol	1.19 (t)	1.00 ± 0.05	0.95 ± 0.19	0.99 ± 0.08[’]	1.30 ± 0.30	1.29 ± 0.12	*0.41*
MCFA	1.33 (br)	1.00 ± 0.11	1.60 ± 0.27	0.75 ± 0.10	3.35 ± 1.31	2.02 ± 0.83	*0.10*

d: doublet, dd: doublet of doublet, t: triplet, s: singulet, m: multiplet, 4-HPPA: 4-Hydroxyphenylacetate, MCFA: medium-chain fatty acids.

[1] P-value of the ANOVA testing the diet effect. a, b, c: P<0.05 after Tukey post-hoc tests. Data are means ± SEM. n=8 rats/group

Table 5. Change in PTP1b level in nodose ganglia after leptin injection in rats fed chow, LF, LF-I, HF/HS or HF/HS-I diets.

	saline	leptin
Chow diet	0.64 ± 0.22	1.46 ± 0.46
LF diet	0.52 ± 0.42	0.71 ± 0.18
LF-I diet	0.76 ± 0.18	0.76 ± 0.26
HF/HS diet	0.58 ± 0.21	0.42 ± 0.09
HF/HS-I diet	1.10 ± 0.17	0.22 ± 0.09 *

Values are means ± SEM (n=2 to 4 rats per group, * P<0.05 compared to saline)